

Tony Kelly · John Church

## The weak bases $\text{NH}_3$ and trimethylamine inhibit the medium and slow afterhyperpolarizations in rat CA1 pyramidal neurons

Received: 12 January 2005 / Accepted: 14 March 2005 / Published online: 27 July 2005  
© Springer-Verlag 2005

**Abstract** The weak bases  $\text{NH}_3$  and trimethylamine (TMeA), applied externally, are widely used to investigate the effects of increasing intracellular pH ( $\text{pH}_i$ ) on neuronal function. However, potential effects of the compounds independent from increases in  $\text{pH}_i$  are not usually considered. In whole-cell patch-clamp recordings from rat CA1 pyramidal neurons, bath application of 1–40 mM  $\text{NH}_4\text{Cl}$  or TMeA HCl reduced resting membrane potential and input resistance, inhibited the medium and slow afterhyperpolarizations (AHPs) and their respective underlying currents,  $mI_{\text{AHP}}$  and  $sI_{\text{AHP}}$ , and led to the development of depolarizing current-evoked burst firing. Examined in the presence of 1  $\mu\text{M}$  TTX and 5 mM TEA with 10 mM Hepes in the recording pipette,  $\text{NH}_3$  and TMeA increased  $\text{pH}_i$  and the magnitudes of depolarization-evoked intracellular  $[\text{Ca}^{2+}]$  transients,  $\text{Ca}^{2+}$ -dependent depolarizing potentials, and inward  $\text{Ca}^{2+}$  currents but reduced the slow AHP and  $sI_{\text{AHP}}$ . When internal  $\text{H}^+$  buffering power was raised by including 100 mM tricine in the patch pipette, the effects of  $\text{NH}_3$  and TMeA to increase  $\text{pH}_i$  and augment  $\text{Ca}^{2+}$  influx were attenuated whereas the reductions in the slow AHP and  $sI_{\text{AHP}}$  (as well as membrane potential and input resistance) were maintained. The findings indicate that increases in  $\text{pH}_i$  contribute to the increases in  $\text{Ca}^{2+}$  influx observed in the presence of  $\text{NH}_3$  and TMeA but not to the reductions in membrane potential, input resistance or the magnitudes of AHPs. The results have implications for the interpretation of data from experiments in which  $\text{pH}_i$  is manipulated by the external application of  $\text{NH}_3$  or TMeA.

**Keywords** Hippocampus · Potassium channels,  $\text{Ca}^{2+}$ -activated · Ammonium · Trimethylamine · Intracellular pH

### Introduction

Extracellular pH ( $\text{pH}_o$ ) is an important modulator of neuronal function [12, 40]. In general, increases in  $\text{pH}_o$  promote and decreases in  $\text{pH}_o$  reduce neuronal excitability, findings which have been interpreted largely in terms of the modulation by  $\text{pH}_o$  of the activities of voltage-gated and ligand-gated ion channels [51, 52]. Less appreciated is the fact that neuronal activity, the application of neurotransmitters and pathophysiological events such as ischemia can all affect intracellular pH ( $\text{pH}_i$ ) [4, 24], with subsequent effects on the activities of ion channels and transport mechanisms for ions such as  $\text{Ca}^{2+}$  and transmitters such as glutamate (e.g. [5, 16, 23, 31, 50]). Furthermore, in many mammalian central neurons,  $\text{pH}_i$  is steeply dependent on  $\text{pH}_o$  [16, 32], raising the possibility that some of the effects of changing  $\text{pH}_o$  on neuronal function may be mediated by changes in  $\text{pH}_i$ .

The medium and slow afterhyperpolarizations (AHPs) which follow a train of action potentials are important determinants of neuronal excitability [41, 42, 53]. Recently we reported that the medium and slow AHPs and their respective underlying currents,  $mI_{\text{AHP}}$  and  $sI_{\text{AHP}}$ , are augmented by increases in  $\text{pH}_o$  [22] (see also [14, 15]). Based on recordings obtained with pipette solutions containing high concentrations of proton buffers, we suggested that a rise in  $\text{pH}_i$  consequent upon the rise in  $\text{pH}_o$  could act to augment the  $\text{Ca}^{2+}$ -activated  $\text{K}^+$  currents that contribute to  $mI_{\text{AHP}}$  and  $sI_{\text{AHP}}$  independently from changes in  $\text{Ca}^{2+}$  influx. To further explore this possibility, in the present study we employed the weak bases  $\text{NH}_3$  ( $\text{pK}_a \sim 9.2$ ) and TMeA ( $\text{pK}_a \sim 9.8$ ) to increase  $\text{pH}_i$  at a constant  $\text{pH}_o$ . In aqueous solutions at physiological pH values, weak bases are incompletely

T. Kelly · J. Church (✉)  
Department of Cellular and Physiological Sciences,  
University of British Columbia, 2177 Wesbrook Mall,  
Vancouver, BC, Canada, V6T 1Z3  
E-mail: jchurch@interchange.ubc.ca  
Tel.: +1-604-8222751  
Fax: +1-604-8222316

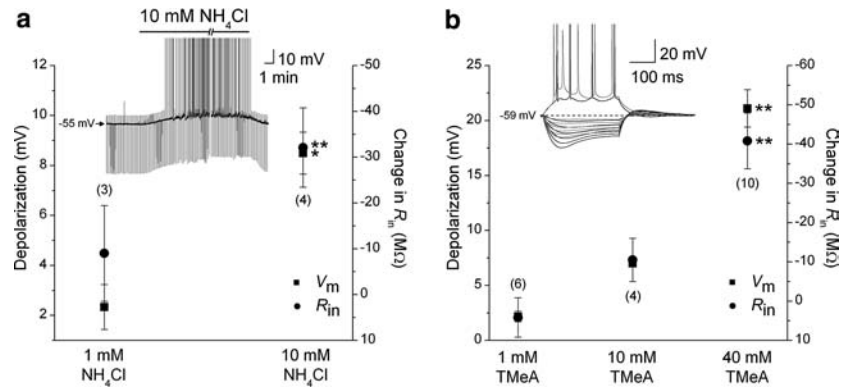


**Fig. 1**  $\text{NH}_3$  and TMeA modulate  $V_m$ ,  $R_{in}$  and repetitive firing properties. All recordings were obtained at  $\text{pH}_o$  7.4 with 10 mM Hepes in the patch pipette. **a** Changes in  $V_m$  (filled square) and  $R_{in}$  (filled circle) observed during the external application of 1 and 10 mM  $\text{NH}_4\text{Cl}$ . Inset typical record of the effects of 10 mM  $\text{NH}_4\text{Cl}$  on  $V_m$  and spontaneous firing; downward deflections are hyperpolarizing potentials elicited by anodal current pulses (0.2 nA, 200 ms, 0.1 Hz). There is a 7 min break in the record. The amplitudes of the spontaneous action potentials seen during the application of  $\text{NH}_4\text{Cl}$  are truncated for convenience in figure preparation. **b** Changes in  $V_m$  (filled square) and  $R_{in}$  (filled circle) observed during the external application of 1, 10 and 40 mM

TMeA. Inset changes in membrane potential elicited by 300 ms hyperpolarizing (from 0.05 to 0.3 nA in 0.05 nA steps) and depolarizing (0.15 nA) current pulses in the absence (continuous line) and presence (dotted line) of 40 mM TMeA; the dashed line indicates  $-59$  mV. Exposure to 40 mM TMeA reduced  $R_{in}$  and changed the pattern of action potential discharge from regular spiking to one in which an initial discharge of three  $\text{Na}^+$ -dependent action potentials was superimposed upon an underlying depolarization. In **a** and **b**, error bars are SEM and  $n$  values are shown in parentheses. \* $P < 0.05$  and \*\* $P < 0.01$  compared to respective control values

dissociated and uncharged molecules rapidly enter cells where they consume protons to increase  $\text{pH}_i$ ; the magnitude of the  $\text{pH}_i$  change depends not only on the concentration and  $\text{pK}_a$  of the weak base applied but also on the total intracellular buffering capacity ( $\beta_T$ ), which is the sum of the intrinsic buffering capacity of the cell and the buffering capacity conferred by the weak base [37, 48].

Contrary to initial expectations, the external application of  $\text{NH}_3$  or TMeA inhibited the medium and slow AHPs and their underlying currents, effects that were independent from increases in  $\text{pH}_i$ . The results emphasize the fact that, although the external application of weak bases affords a convenient way to increase  $\text{pH}_i$  at a constant  $\text{pH}_o$ , these compounds can modulate neuronal function separate from their effects on  $\text{pH}_i$ .

## Materials and methods

### Experimental tissue

All procedures conformed to guidelines established by the Canadian Council on Animal Care and were approved by The University of British Columbia Animal Care Committee. Transverse hippocampal slices (400  $\mu\text{m}$ ), prepared from a total of thirty-eight 17–23-day-old Wistar rats as described previously [15], were used for the majority of the experiments. In brief, animals were anaesthetized with 3% halothane in air, decapitated and the brains rapidly removed. Slices were then prepared and allowed to recover for at least 1 h at room temperature (RT, 19–23°C) before being transferred as needed to a recording chamber, where they

were placed at the interface between a humidified 5%  $\text{CO}_2/95\%$   $\text{O}_2$  atmosphere and a continuously (2 ml  $\text{min}^{-1}$ ) superfusing medium. Simultaneous measurements of  $\text{pH}_i$  and intracellular free calcium concentration ( $[\text{Ca}^{2+}]_i$ ) were performed in hippocampal neurons obtained from 2- to 4-day old postnatal Wistar rats and placed in primary culture as described [39]. Cultured neurons (from five different batches of cultures) were used 8–14 days after plating.

### Solutions and chemicals

The standard bath solution contained (mM) NaCl 123, KCl 3,  $\text{NaHCO}_3$  26,  $\text{NaH}_2\text{PO}_4$  1.5,  $\text{MgSO}_4$  1.5, D-glucose 10 and  $\text{CaCl}_2$  2 (pH 7.4 after equilibration with 5%  $\text{CO}_2/95\%$   $\text{O}_2$ ). Solutions containing 1–40 mM  $\text{NH}_4\text{Cl}$ , trimethylamine HCl (TMeA) or *p*-aminobenzoic acid diethylaminoethyl ester HCl (procaine) were prepared by equimolar substitution for NaCl. Patch pipettes were filled with a solution containing either a standard or a high concentration of  $\text{H}^+$  buffer. The standard pipette solution contained (mM)  $\text{KMeSO}_4$  140, KCl 7,  $\text{MgCl}_2$  3,  $\text{K}_2\text{-ATP}$  2 and Hepes 10 (titrated to pH 7.3 with 6 mM KOH); the high  $\text{H}^+$  buffer pipette solution contained (mM)  $\text{KMeSO}_4$  85, KCl 7,  $\text{MgCl}_2$  3,  $\text{K}_2\text{-ATP}$  2, and *N*-[tris(hydroxymethyl)methyl]glycine (tricine) 100 (titrated to pH 7.3 with 37 mM KOH); final osmolarity was  $\sim 290$  mosmol  $\text{l}^{-1}$ . Experiments were performed at RT.

Salts and experimental compounds were obtained from Sigma–Aldrich Canada Ltd. (Oakville, ON, Canada), with the exceptions of potassium methylsulphate (ICN Pharmaceuticals Canada Ltd., Montréal, QC,

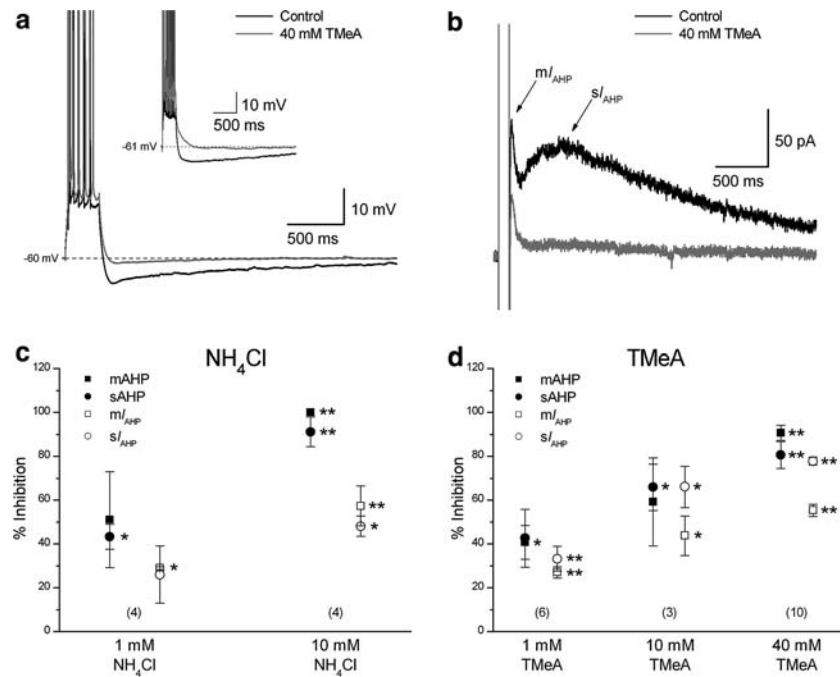


**Fig. 2** NH<sub>3</sub> and TMeA inhibit medium and slow AHPs and their underlying currents. All recordings were obtained at pH<sub>o</sub> 7.4 with 10 mM internal Hepes. **a** Under control conditions, a 300 ms depolarizing current-evoked train of action potentials was followed by medium and slow AHPs. The addition of 40 mM TMeA inhibited the AHPs, which, in two out of ten cells, were replaced by an ADP (*inset*). **b** Under control conditions, a 100 ms depolarizing step from -50 to 20 mV was followed by the temporally distinct outward currents m<sub>I</sub>AHP and s<sub>I</sub>AHP. Both currents were reduced in

the presence of 40 mM TMeA. **c, d** Summaries of the effects of NH<sub>4</sub>Cl (**c**) and TMeA (**d**), applied at the concentrations shown on the figure, on the medium AHP (*filled square*; mAHP), slow AHP (*filled circle*; sAHP) and the respective underlying currents, m<sub>I</sub>AHP (*open square*) and s<sub>I</sub>AHP (*open circle*), expressed as percentage inhibitions of peak amplitudes observed in the same cells under control conditions. Error bars are SEM and *n* values are shown in parentheses. \**P* < 0.05 and \*\**P* < 0.01 compared to respective measurements made under control conditions

Canada), tetrodotoxin (TTX; Alomone Labs Ltd., Jerusalem, Israel), and fura-2 (pentapotassium salt) and SNARF-5F (acetoxymethyl ester (AM) form) (Molecular Probes Inc., Eugene, OR, USA).

### Recording techniques

In the majority of experiments, conventional whole-cell patch pipette current-clamp and voltage-clamp recordings were obtained from CA1 neurons in hippocampal slices using the 'blind' technique. Patch pipettes were pulled from 1.2 mm o.d. × 0.9 mm i.d. borosilicate tubing (World Precision Instruments Inc., Sarasota, FL, USA) and heat-polished; open pipette resistance when filled was 2–5 MΩ. After a seal >1 GΩ was achieved, recordings were made (Axoclamp 2, Axon Instruments Inc., Union City, CA, USA) when the application of light suction revealed a membrane potential (*V<sub>m</sub>*) of at least -55 mV (after subtraction of the 5–7 mV junction and tip potentials; [34]), overshooting action potentials, an input resistance (*R<sub>in</sub>*) > 100 MΩ and a stable series resistance (8–30 MΩ). The reference bath electrode was a 3 M KCl, 4% agar bridge. Voltage-waveforms and current-waveforms were low-pass filtered at 2.7 and 1.2 kHz, respectively, and digitized at 5–10 kHz using a

Digidata 1200 controlled by pCLAMP software (Version 6, Axon Instruments Inc.). Leakage currents were subtracted off-line.

Concurrent measurements of pH<sub>i</sub> and [Ca<sup>2+</sup>]<sub>i</sub> were performed in whole-cell patch-clamped cultured hippocampal neurons using the pH indicator SNARF-5F and the Ca<sup>2+</sup> indicator fura-2 (see [26]). To load SNARF-5F, coverslips with neurons attached were placed in standard perfusion medium containing 10 μM SNARF-5F-AM for 30 min at 34°C, after which coverslips were placed in standard medium for 20 min to ensure de-esterification of the fluorophore. Fura-2 loading was achieved by including 100 μM fura-2 pentapotassium salt in the patch pipette solution. After establishing the whole-cell configuration, ≥10 min was allowed for the diffusion of fura-2 into the neuron; measurements of pH<sub>i</sub> and [Ca<sup>2+</sup>]<sub>i</sub> were then collected continuously by alternating between the dual-emission and dual-excitation modes. As detailed in Sheldon et al. [39], fura-2-derived fluorescence emission intensities were measured with a single camera at 550 nm during excitation at 334 nm and then at 380 nm; the excitation wavelength was then changed to 488 nm and SNARF-5F-derived fluorescence emissions were split by a dichroic mirror centered at 605 nm and measured by two separate cameras at 550 and 640 nm. Each automated cycle took ~1.5 s to

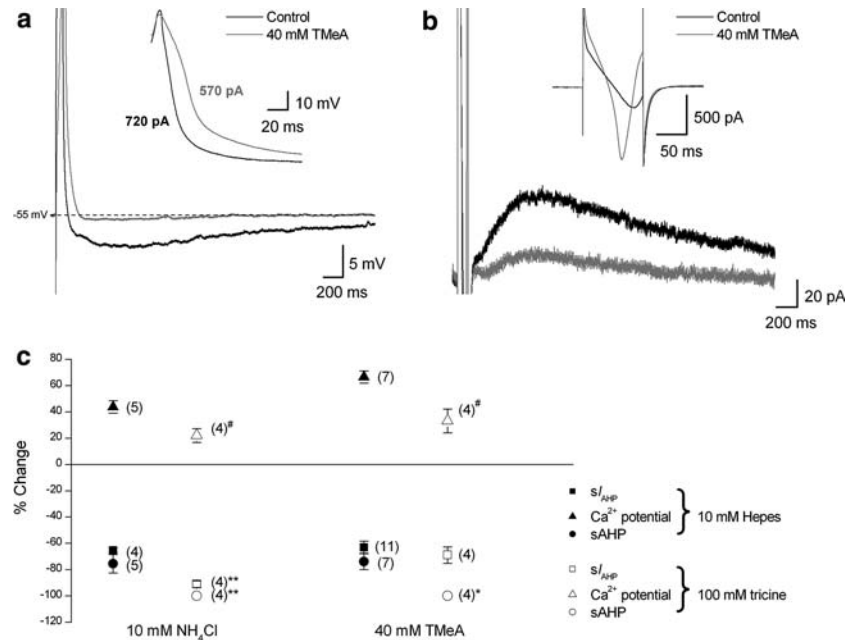


**Fig. 3** NH<sub>3</sub> and TMeA increase Ca<sup>2+</sup> influx but inhibit the slow AHP and s I<sub>AHP</sub>. All records were obtained at pH<sub>o</sub> 7.4 in the presence of 1 μM TTX and 5 mM TEA. **a**, **b** Recordings from the same CA1 neuron under **a** current-clamp and **b** voltage-clamp conditions; the patch pipette contained 10 mM Hepes. **a** Compared to control conditions, the application of 40 mM TMeA increased the half-amplitude duration of the Ca<sup>2+</sup>-dependent depolarizing potential (*inset*) and decreased the peak amplitude of the subsequent slow AHP. The magnitudes of the 60 ms depolarizing current pulses employed to elicit the Ca<sup>2+</sup> potential under control and test conditions are shown on the figure. **b** Compared to control conditions, 40 mM TMeA increased the partially clamped I<sub>Ca</sub> elicited by a 100 ms step from -50 to 0 mV (*inset*) and decreased

the amplitude of the subsequent s I<sub>AHP</sub>. **c** Summaries of effects of 10 mM NH<sub>4</sub>Cl and 40 mM TMeA on the half-amplitude durations of Ca<sup>2+</sup> potentials (*solid triangles*), the peak amplitudes of the subsequent slow AHPs (*solid circles*), and s I<sub>AHP</sub>s (*solid squares*) recorded with 10 mM internal Hepes. Also shown are the effects of the same experimental manoeuvres recorded with 100 mM internal Tricine (*open symbols*). Results are expressed as percentage changes from control values established in the absence of a weak base. Error bars are SEM and *n* values are shown in *parentheses*. \**P* < 0.05 and \*\**P* < 0.01 for the difference between the corresponding measurements obtained with 10 mM internal Hepes and 100 mM internal Tricine. #*P* < 0.05 for the difference between the corresponding percentage change obtained with 10 mM internal Hepes

complete and was repeated every 2–15 s during the course of an experiment.

#### Experimental procedures and data analysis

In current-clamp recordings, the effects of changes in perfusate composition on *V<sub>m</sub>*, *R<sub>in</sub>* and the amplitudes of the medium and slow AHPs which followed a 300 ms depolarizing current-evoked train of action potentials were quantified as described [14]. The magnitude of the depolarizing current pulse employed to evoke the spike train was varied to elicit the same number of action potentials under control and test conditions. Test measurements of *R<sub>in</sub>* and medium and slow AHP amplitudes were conducted at the original control membrane potential by passing, when necessary, steady current through the recording electrode. In experiments conducted in the presence of 1 μM TTX and 5 mM tetraethylammonium (TEA), a 40–100 ms depolarizing current pulse was employed to elicit a Ca<sup>2+</sup>-dependent depolarizing potential that was followed by a slow AHP; the half-amplitude duration of the Ca<sup>2+</sup> potential and the peak amplitude of the subsequent slow AHP were measured (see [14, 22]). Under test conditions where a

spike train evoked an afterdepolarization (ADP), this was taken as 100% inhibition of the medium and slow AHPs.

Under voltage-clamp conditions, 80–200 ms depolarizing voltage steps from the holding potential (-50 mV) to 0–20 mV elicited partially clamped inward currents that were followed by early (mI<sub>AHP</sub>) and late (sI<sub>AHP</sub>) outward K<sup>+</sup> currents. Experimentally induced changes in mI<sub>AHP</sub> and sI<sub>AHP</sub> were quantified by comparing the peak amplitudes of the currents obtained under control and test conditions; if a distinct peak was not evident under a test condition, current amplitude was compared isochronally to the peak of the appropriate current measured under control conditions. In the presence of 1 μM TTX and 5 mM TEA, the depolarizing voltage step elicited a robust Co<sup>2+</sup>-sensitive and nifedipine-sensitive inward Ca<sup>2+</sup> current (I<sub>Ca</sub>; see [22]) that was followed by a sI<sub>AHP</sub>; the I<sub>Ca</sub>s evoked under control and test conditions were compared qualitatively whereas the peak amplitudes of the subsequent sI<sub>AHP</sub>s were measured and compared statistically.

In microspectrofluorimetric experiments, the one-point nigericin/high-[K<sup>+</sup>] technique was employed to convert background-corrected SNARF-5F-derived emission intensity ratios (*BI*<sub>550</sub>/*BI*<sub>640</sub>) into pH<sub>i</sub> values as

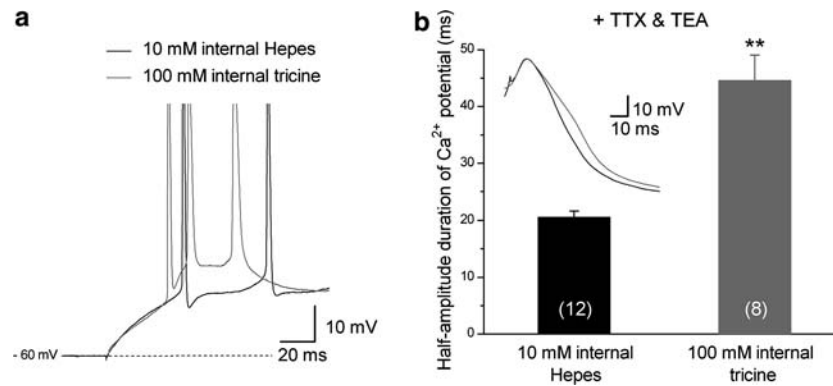


**Fig. 4** Increasing  $\beta_T$  with 100 mM internal tricaine modulates the pattern of action potential discharge and depolarizing  $\text{Ca}^{2+}$  potentials. Current-clamp recordings were obtained at  $\text{pH}_o$  7.4. **a** Typical records of the patterns of action potential discharge observed in response to depolarizing current injection recorded with 10 mM internal HEPES and 100 mM internal tricaine ( $V_m$ ,  $-60$  mV). Action potential amplitudes are truncated at this voltage

gain. **b** The half-amplitude duration of the  $\text{Ca}^{2+}$  potential evoked by a 60 ms depolarizing current pulse in the presence of  $1 \mu\text{M}$  TTX and 5 mM TEA (*inset*) was significantly (\*\* $P < 0.01$ ) greater when recorded with 100 mM internal tricaine compared to 10 mM internal HEPES. Error bars are SEM and  $n$  values are shown in parentheses

described [39]. The  $\text{pH}_i$  value measured immediately prior to a  $[\text{Ca}^{2+}]_i$  transient evoked by a 200 ms depolarizing voltage step from  $-70$  to  $20$  mV was employed to correct the  $K_d$  of fura-2 for  $\text{Ca}^{2+}$  according to Martínez-Zaguilán et al. [27] (see also [16]). The magnitudes of pH-corrected  $[\text{Ca}^{2+}]_i$  transients under control and test conditions were measured by numerical integration and are presented in nM·s.

To allow  $\text{pH}_i$  to reach a new steady-state level, test responses were elicited  $> 10$  min (slice preparations) and  $> 3$  min (cultured neurons) after the introduction of a weak base (e.g. see Fig. 5). Full recovery from the effects of a weak base on  $\text{Ca}^{2+}$  potentials, AHPs and their underlying currents was slow and usually only observed with lower concentrations (i.e. 1–10 mM  $\text{NH}_4\text{Cl}$  or TMeA). In these cases, the effects of a weak base were quantified by comparing the magnitude of the test response with the magnitude of the computed mean of the control and recovery responses. Only if full recovery was obtained were the effects of a second application of a weak base examined.

Data were analyzed in pCLAMP Version 6 and Origin Version 7 (OriginLab Corp., Northampton, MA, USA) and are presented as means  $\pm$  SEM, with the accompanying  $n$  value referring to the number of neurons from which data were obtained. Statistical comparisons were performed using Student's two-tailed  $t$ -test, paired or unpaired as appropriate, with a 95% confidence limit.

## Results

### Effects of $\text{NH}_3$ and TMeA on passive membrane and repetitive firing properties

In agreement with previous findings in a variety of invertebrate (e.g. [7, 45]) and vertebrate (e.g. [6, 19, 46,

50]) neurons, exposure to 1–10 mM  $\text{NH}_4\text{Cl}$  (Fig. 1a) or 1–40 mM TMeA (Fig. 1b) produced concentration-dependent reductions in  $V_m$  and  $R_{in}$  and frequently led to the development of spontaneous activity (see Fig. 1a, *inset*). The application of 40 mM TMeA, for example, reduced  $V_m$  from  $-58 \pm 1$  to  $-37 \pm 2$  mV and decreased  $R_{in}$  from  $134 \pm 9$  to  $93 \pm 8 \text{ M}\Omega$  ( $n = 10$  and  $P < 0.01$  in each case). Applied at  $\geq 10$  mM,  $\text{NH}_4\text{Cl}$  and TMeA also altered the pattern of action potential discharge in response to 300 ms depolarizing current pulses. For example, as shown in Fig. 1b (*inset*), in seven of nine neurons which exhibited a regular spiking discharge under control conditions, exposure to 40 mM TMeA lead to the development of an initial discharge of 2–6 fast  $\text{Na}^+$ -dependent action potentials superimposed upon a slow depolarization (“burst-firing” neurons; see [3, 15]).

### Effects of $\text{NH}_3$ and TMeA on $\text{Ca}^{2+}$ potentials and medium and slow AHPs

In rat CA1 neurons, increases in  $\text{pH}_o$  and/or  $\text{pH}_i$  augment  $\text{Ca}^{2+}$  influx and the medium and slow AHPs [14, 15, 22, 50, 51]. Therefore, we examined the effects of the external application of weak bases on  $\text{Ca}^{2+}$ -dependent depolarizing potentials, inward  $\text{Ca}^{2+}$  currents, and the medium and slow AHPs and their underlying currents.

Under control conditions, 300 ms depolarizing current pulses elicited trains of action potentials that were followed by medium and slow AHPs of  $4.5 \pm 0.3$  and  $4.3 \pm 0.4$  mV, respectively ( $n = 27$  in each case; Fig. 2a). Under voltage-clamp conditions, 80–200 ms depolarizing steps from  $-50$  to  $0$ – $20$  mV generated two temporally distinct outward currents (Fig. 2b; see also [22]). The early current,  $mI_{AHP}$ , which receives contributions from both an apamin-sensitive  $\text{Ca}^{2+}$ -activated  $\text{K}^+$  current ( $I_{AHP}$ ) and a muscarine-sensitive voltage-gated  $\text{K}^+$  current ( $I_M$ ), had a peak amplitude of  $114 \pm 9 \text{ pA}$

( $n=43$ ); the late current,  $sI_{\text{AHP}}$ , is mediated by apamin-insensitive  $\text{Ca}^{2+}$ -activated  $\text{K}^+$  channels and had a peak amplitude of  $83 \pm 7$  pA ( $n=43$ ). Surprisingly, in light of their effect to increase  $\text{pH}_i$  and  $\text{Ca}^{2+}$  influx (see below),  $\text{NH}_4\text{Cl}$  (1–10 mM) and TMeA (1–40 mM) inhibited the medium and slow AHPs and their underlying current(s) (Fig. 2). For example, 40 mM TMeA reduced the amplitude of the medium AHP from  $4.4 \pm 0.3$  to  $0.4 \pm 0.2$  mV and the slow AHP from  $4.4 \pm 0.7$  to  $0.9 \pm 0.3$  mV ( $n=10$  and  $P < 0.01$  in each case); in two neurons, inhibition of the AHPs was associated with the development of an ADP (Fig. 2a, inset). Corresponding changes were seen in  $mI_{\text{AHP}}$  and  $sI_{\text{AHP}}$ , which decreased from  $133 \pm 32$  and  $108 \pm 14$  pA, respectively, under control conditions to  $57 \pm 10$  and  $25 \pm 5$  pA, respectively, in the presence of 40 mM TMeA ( $n=10$  and  $P < 0.01$  in each case). The decreases in  $mI_{\text{AHP}}$  induced by the weak bases cannot be fully accounted for by concomitant reductions in  $sI_{\text{AHP}}$  which, under our experimental conditions, contributes to  $\sim 15\%$  of the peak amplitude of  $mI_{\text{AHP}}$  (see [22]).

As illustrated in Fig. 3, the inhibition of the slow AHP and  $sI_{\text{AHP}}$  by  $\text{NH}_3$  and TMeA was not due to a reduction in  $\text{Ca}^{2+}$  influx through the high-voltage-activated  $\text{Ca}^{2+}$  channels that are the primary source of  $\text{Ca}^{2+}$  for their activation (see [38]). Examined in the presence of 1  $\mu\text{M}$  TTX and 5 mM TEA, 40 mM TMeA significantly ( $P < 0.01$ ) increased the half-amplitude duration of the  $\text{Co}^{2+}$ -sensitive and nifedipine-sensitive  $\text{Ca}^{2+}$ -dependent depolarizing potential evoked by a 40–100 ms depolarizing current pulse (see [14]) from  $22 \pm 1$  to  $36 \pm 2$  ms ( $n=7$ ); in the same cells, the amplitude of the subsequent slow AHP declined significantly ( $P < 0.01$ ) from  $6.4 \pm 0.6$  to  $1.7 \pm 0.4$  mV (Fig. 3a, c). Qualitatively similar results were obtained with 10 mM (Fig. 3c) and 40 mM (not shown)  $\text{NH}_4\text{Cl}$ . Under voltage-clamp conditions,  $I_{\text{Ca}}$  was augmented by the addition of 1  $\mu\text{M}$  TTX and 5 mM TEA, at which time the amplitude of  $sI_{\text{AHP}}$  increased from  $64 \pm 9$  to  $100 \pm 9$  pA ( $n=15$ ;  $P < 0.01$ ). Consistent with results obtained under current-clamp conditions (see also [50]), the subsequent application of 40 mM TMeA ( $n=11$ ) further increased  $I_{\text{Ca}}$  whereas  $sI_{\text{AHP}}$  measured in the same neurons declined significantly ( $P < 0.01$ ) from  $89 \pm 9$  to  $30 \pm 3$  pA (Fig. 3b, c). Comparable results were obtained with 10 mM (Fig. 3c) and 40 mM (not shown)  $\text{NH}_4\text{Cl}$ . Application of 40 mM procaine ( $\text{pK}_a \sim 8.9$ ) also significantly ( $P < 0.05$ ) inhibited  $sI_{\text{AHP}}$  by  $89 \pm 14\%$  ( $n=3$ ; see also [20]); in the same neurons, however, procaine decreased  $I_{\text{Ca}}$  (see also [43]) suggesting that, in contrast to  $\text{NH}_3$  and TMeA, reduced  $\text{Ca}^{2+}$  influx contributes to the ability of procaine to inhibit  $sI_{\text{AHP}}$ .

#### Effects of $\text{NH}_3$ and TMeA recorded with high internal $\text{H}^+$ buffering capacity

To investigate the role of increases in  $\text{pH}_i$  in the aforementioned effects of  $\text{NH}_3$  and TMeA,  $\beta_T$  was increased

by including 100 mM tricine in the patch pipette; tricine was employed because internal concentrations of Hepes and structurally related buffers  $\geq 50$  mM inhibit  $mI_{\text{AHP}}$  and  $sI_{\text{AHP}}$  [22].

In contrast to recordings made with 10 mM internal Hepes in the absence of  $\text{NH}_3$  or TMeA, where a total of 4 out of 27 neurons exhibited an initial weak burst of action potentials in response to a 300 ms depolarizing current pulse, weak burst firing was observed in 6 out of 8 cells with 100 mM internal tricine (Fig. 4a). This observation may reflect the finding that, in agreement with Tombaugh [49], the half-amplitude duration of the depolarizing  $\text{Ca}^{2+}$  potential recorded with 100 mM internal tricine in the presence of 1  $\mu\text{M}$  TTX and 5 mM TEA was significantly greater than that observed with 10 mM internal Hepes (Fig. 4b). Also in agreement with Tombaugh [49], the amplitude of the subsequent slow AHP recorded with 100 mM internal tricine ( $5.7 \pm 0.5$  mV,  $n=8$ ) tended to be greater than that observed with 10 mM internal Hepes ( $5.0 \pm 0.4$  mV,  $n=12$ ), although this effect did not reach statistical significance.

The inclusion of 100 mM tricine in the patch pipette did not significantly affect the reductions in  $V_m$  or  $R_{\text{in}}$  evoked by 10 mM  $\text{NH}_4\text{Cl}$  or 40 mM TMeA (not shown). In addition, with 100 mM internal tricine, the application of 10 mM  $\text{NH}_4\text{Cl}$  or 40 mM TMeA continued to augment depolarization-evoked  $\text{Ca}^{2+}$  potentials recorded in the presence of 1  $\mu\text{M}$  TTX and 5 mM TEA; reminiscent of the findings of Tombaugh and Somjen [50], however, the increases were significantly less than those observed with 10 mM internal Hepes (Fig. 3c). Furthermore, the reductions in the slow AHP induced by 10 mM  $\text{NH}_4\text{Cl}$  and 40 mM TMeA were significantly enhanced in the presence of 100 mM internal tricine compared to 10 mM internal Hepes (Fig. 3c). For example, examined in four cells with 100 mM internal tricine, 40 mM TMeA blocked the slow AHP which, in two of the cells, was replaced by a slow ADP. Comparable results were obtained under voltage-clamp conditions with 100 mM internal tricine, where 10 mM  $\text{NH}_4\text{Cl}$  and 40 mM TMeA increased  $I_{\text{Ca}}$  ( $n=4$  cells in each case) and continued to reduce  $sI_{\text{AHP}}$  (Fig. 3c). Qualitatively similar effects were seen with 40 mM  $\text{NH}_4\text{Cl}$  (not shown).

#### Effects of $\text{NH}_3$ and TMeA on $\text{pH}_i$ and depolarization-evoked $[\text{Ca}^{2+}]_i$ transients

The results obtained with 100 mM internal tricine suggest that an increase in  $\text{pH}_i$  contributes to the increase in  $\text{Ca}^{2+}$  influx but not to the reduction in the slow AHP and  $sI_{\text{AHP}}$  induced by  $\text{NH}_3$  and TMeA. Therefore, in the final series of experiments, we examined the effect of increasing  $\beta_T$  on the changes in  $\text{pH}_i$  and depolarization-evoked  $[\text{Ca}^{2+}]_i$  transients induced by 40 mM TMeA in cultured hippocampal neurons.

Resting  $\text{pH}_i$  measured in whole-cell patch-clamped neurons was significantly higher with 100 mM tricine compared to 10 mM Hepes in the recording pipette (Table 1). The deviation of the measured resting  $\text{pH}_i$  from the pipette  $\text{pH}$ , and the difference in resting  $\text{pH}_i$  between neurons patch-clamped with pipette solutions of the same  $\text{pH}$  but differing buffering capacity, are entirely consistent with previous reports in a variety of cell types patch-clamped in the whole-cell configuration (e.g. [10, 17, 18]). As detailed in Table 1 and shown in Fig. 5, the inclusion of 100 mM tricine in the patch pipette significantly blunted the increase in  $\text{pH}_i$  evoked

by the external application of 40 mM TMeA. Higher concentrations of tricine could not be employed to abolish the weak-base-induced increases in  $\text{pH}_i$  because they inevitably lead to unacceptable reductions in internal  $[\text{K}^+]_i$  (see [22]) and frequently cause large increases in series resistance (T. Kelly and J. Church, unpublished observations). In the absence of TMeA, resting  $[\text{Ca}^{2+}]_i$  was not significantly different ( $P > 0.9$ ) in neurons whole-cell patch-clamped with 10 mM internal Hepes or 100 mM internal tricine (Table 1). Reminiscent of the increase in the half-amplitude duration of  $\text{Ca}^{2+}$ -dependent depolarizing potentials observed with

**Table 1**  $\text{pH}_i$  and  $[\text{Ca}^{2+}]_i$  in patch-clamped and intact neurons in the absence and presence of 40 mM TmeA

		10 mM internal Hepes	Intact	100 mM internal tricine	Intact
+ TMeA	Resting $\text{pH}_i$ (pH units)	$7.00 \pm 0.04$ (11)	$7.12 \pm 0.04$	$7.20 \pm 0.04$ (10)*	$7.13 \pm 0.07$
	Resting $[\text{Ca}^{2+}]_i$ (nM)	$88 \pm 13$ (7)		$87 \pm 12$ (7)	
	$[\text{Ca}^{2+}]_i$ transient (nM·s)	$433 \pm 123$ (5)		$690 \pm 100$ (5)	
+ TMeA	Increase in $\text{pH}_i$ (pH units)	$0.55 \pm 0.03$ (11)	$0.37 \pm 0.02$	$0.20 \pm 0.02$ (10)**	$0.40 \pm 0.02$
	Steady-state $[\text{Ca}^{2+}]_i$ (nM)	$79 \pm 12$ (7)		$97 \pm 15$ (7)	
	$[\text{Ca}^{2+}]_i$ transient (nM·s)	$703 \pm 184$ (5)		$821 \pm 123$ (5)	

For neurons patch-clamped with the indicated concentration of  $\text{H}^+$  buffer in the pipette,  $n$  values (shown in *parentheses*) indicate the number of neurons, each on a different coverslip, from which data were obtained. The  $\text{pH}_i$  measurements obtained simultaneously from intact (*unpatched*) neurons on the same coverslips ( $n > 50$  in all cases) are presented in the adjacent columns  
\* $P < 0.05$  and \*\* $P < 0.01$  for the difference to the respective value obtained with 10 mM internal Hepes

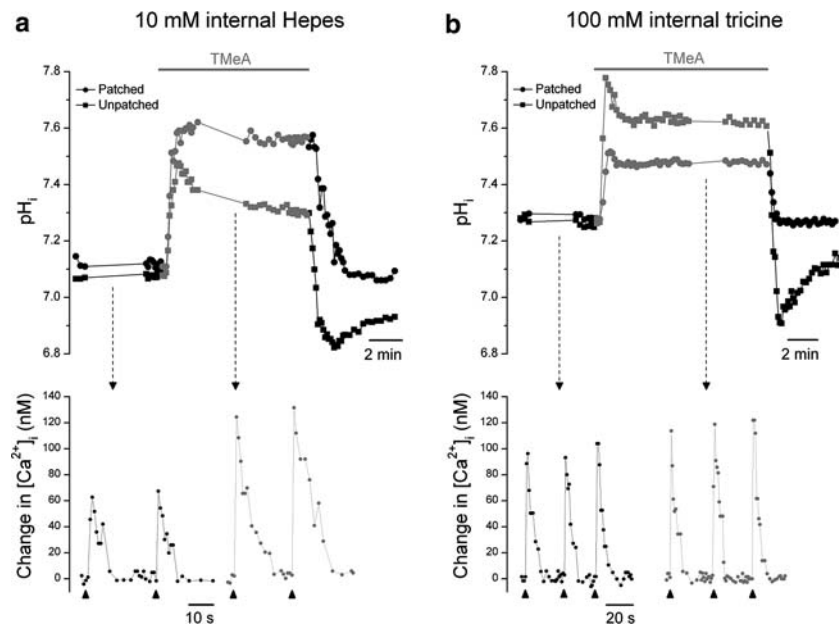


**Fig. 5** Effects of increasing  $\beta_r$  on 40 mM TMeA-induced changes in  $\text{pH}_i$  and depolarization-evoked  $[\text{Ca}^{2+}]_i$  transients. All records were obtained at  $\text{pH}_o$  7.4 in the presence of 1  $\mu\text{M}$  TTX and 5 mM TEA. **a** In a hippocampal neuron co-loaded with fura-2 and SNARF-5F and patch-clamped in the whole-cell configuration with 10 mM Hepes in the pipette, the application of 40 mM TMeA evoked a rise in  $\text{pH}_i$  (filled circles). Also shown is the  $\text{pH}_i$  response to TMeA recorded simultaneously in an unpatched neuron on the same coverslip (filled squares). The lack of an internal acidification upon the removal of TMeA in

the patch-clamped cell (*cf* the intact neuron) is consistent with previous reports (e.g. [23]). Beneath the  $\text{pH}_i$  records are shown the increases in  $[\text{Ca}^{2+}]_i$  evoked in the patched cell by 200 ms depolarizing voltage steps from  $-70$  to  $20$  mV (applied at the *small arrows*), both prior to and during the application of TMeA. **b** Records from a similar experiment to that illustrated in **a** but in which the recording pipette used to patch-clamp the neuron contained 100 mM tricine. In **a** and **b**, the acquisition of  $\text{pH}_i$  data was interrupted during the recording of  $[\text{Ca}^{2+}]_i$  transients

high  $\beta_T$  (see above), the magnitude of  $[Ca^{2+}]_i$  transients evoked by 200 ms depolarizing voltage steps from  $-70$  to  $20$  mV tended to be greater with 100 mM internal tricine compared to 10 mM internal Hepes, although the increase failed to reach statistical significance ( $P=0.07$ ; Table 1). As reported previously for  $NH_4Cl$  [29, 33], exposure to 40 mM TMeA often elicited an immediate increase in  $[Ca^{2+}]_i$  ( $41 \pm 17$  nm in four out of seven cells with 10 mM internal Hepes and  $38 \pm 8$  nm in five out of seven cells with 100 mM internal tricine) which rapidly ( $<2$  min) returned to resting levels; thereafter, steady-state  $[Ca^{2+}]_i$  in the presence of 40 mM TMeA was not significantly different ( $P>0.4$ ) with 10 mM internal Hepes versus 100 mM internal tricine (Table 1). In contrast, coincident with the reduction in the magnitude of the TMeA-induced increase in  $pH_i$  observed in the presence of 100 mM internal tricine compared to 10 mM internal Hepes, the increase in the magnitude of depolarization-evoked  $[Ca^{2+}]_i$  transients observed in the presence of 40 mM TMeA was limited to  $19 \pm 3\%$  by 100 mM internal tricine ( $P<0.01$  compared to the  $62 \pm 12\%$  increase observed in the presence of 10 mM Hepes) (Table 1; Fig. 5).

## Discussion

Exposure to weak bases is widely employed to study the effects of increases in  $pH_i$  on cell function independent from changes in  $pH_o$ , but the possibility that these compounds might modulate neuronal activity independent from their effects on  $pH_i$  is usually ignored. In the present study, although  $NH_3$  and TMeA exerted a number of effects on hippocampal neuron excitability, only the weak-base-induced augmentation of  $Ca^{2+}$  influx was attenuated by increasing internal  $H^+$  buffering capacity; in contrast, the effects of  $NH_3$  and TMeA to reduce  $V_m$  and  $R_{in}$  and inhibit the slow and, possibly, medium AHPs and their underlying currents appeared unrelated to changes in  $pH_i$ .

The pronounced membrane depolarization seen upon the application of  $NH_3$  or TMeA was not affected by increasing  $\beta_T$ , suggesting that the effect was not mediated by an increase in  $pH_i$ . Rather, the reduction in  $V_m$  may reflect the entry of the protonated form of a weak base through  $K^+$  and/or non-selective cation channels [25, 46], with an additional contribution arising from the inhibition of  $mI_{AHP}$  and  $sI_{AHP}$ . In contrast, the effects of  $NH_3$  and TMeA to increase the magnitudes of depolarization-evoked  $Ca^{2+}$  potentials,  $[Ca^{2+}]_i$  transients and  $I_{Ca}$  were attenuated by increasing  $\beta_T$ . Although these findings are consistent with reports that increases in  $pH_i$  augment  $Ca^{2+}$  influx via high-voltage-activated  $Ca^{2+}$  channels [23, 28, 47, 50], the attenuation of the enhanced  $Ca^{2+}$  influx by high  $\beta_T$  was not complete. This may in part reflect the inability of 100 mM internal tricine to abolish the rise in  $pH_i$  evoked by a high concentration of TMeA, although effects independent from increases in  $pH_i$  also likely contribute. Two possibilities

of immediate relevance to the present study are increases in internal  $H^+$  buffering capacity and/or reductions in the medium and slow AHPs induced by weak bases.

In interneurons of the CA1 region, increasing  $\beta_T$  enhances  $Ca^{2+}$  influx, an effect suggested to reflect a blunting of activity-induced reductions in  $pH_i$ , which would normally act to limit  $Ca^{2+}$  entry through high-voltage-activated  $Ca^{2+}$  channels [49] (see also [54]). Indeed, in the present study, depolarization-induced  $Ca^{2+}$  potentials and  $[Ca^{2+}]_i$  transients recorded with 100 mM internal tricine were larger than those recorded with 10 mM internal Hepes, an effect which may contribute to the increased propensity to burst firing with 100 mM internal tricine even in the absence of a weak base [14, 15, 21, 55]. Because externally applied weak bases markedly increase total intracellular  $H^+$  buffering power [44], increases in  $\beta_T$  could contribute to the augmentation of  $Ca^{2+}$  potentials,  $[Ca^{2+}]_i$  transients (and burst firing) by  $NH_3$  and TMeA. An additional possibility is that weak-base-induced increases in  $Ca^{2+}$  influx could in part reflect the inhibition of the medium and slow AHPs, which normally act as a negative feedback mechanism to regulate  $Ca^{2+}$  influx [11, 13, 16, 30]. This could also provide an explanation for previous findings that externally applied weak bases have a greater effect to augment  $Ca^{2+}$ -dependent depolarizing potentials (evoked under conditions where AHPs were not blocked) than  $I_{Ca}$  (evoked under conditions where all  $K^+$  currents were blocked) [47] (see also [50]). Inhibition of  $mI_{AHP}$  and  $sI_{AHP}$ , with a consequent increase in  $Ca^{2+}$  influx and decrease in  $K^+$  efflux, may also contribute to the development of the ADPs occasionally seen in the presence of  $NH_3$  or TMeA [36, 56, 57].

The weak-base-induced inhibition of the slow AHP and  $sI_{AHP}$  observed in the face of increased  $Ca^{2+}$  influx was not attenuated by 100 mM internal tricine, indicating that  $NH_3$  and TMeA inhibit the slow AHP and its underlying current independent from changes in  $pH_i$  and downstream from  $Ca^{2+}$  influx. (Although we did not examine whether the weak-base-induced inhibition of the medium AHP and  $mI_{AHP}$  might also be independent from changes in  $pH_i$ , we have previously shown that the medium AHP and  $mI_{AHP}$ , like the slow AHP and  $sI_{AHP}$ , are augmented by increases in  $pH_i$ , effects that are mediated in large part by an increase in the apamin-sensitive  $Ca^{2+}$ -activated  $K^+$  current,  $I_{AHP}$  [22].) While the precise mechanism(s) underlying the weak-base-induced inhibition of the medium and slow AHPs remain unknown, weak bases could, for example, affect the  $Ca^{2+}$ -sensing of the  $Ca^{2+}$ -activated  $K^+$  channels underlying  $I_{AHP}$  and  $sI_{AHP}$  (see [8]), decrease the  $K^+$  equilibrium potential by depleting intracellular  $K^+$  (see [19]) and/or interact directly with the channels underlying the medium and slow AHPs to inhibit their activities. The latter could, for example, involve the protonated forms of  $NH_3$  and TMeA acting via an internal site, in a manner analogous to the block of SK2 channels (which mediate  $I_{AHP}$ ) by intracellular quaternary amines [9] and the inhibition of the slow

AHP in rat CA1 pyramidal neurons by the weak base ( $pK_a \sim 9.2$ ) 4-aminopyridine (4-AP) [1] (see also [2]). Similar to the effects of  $NH_3$  and TMeA reported here, the low millimolar concentrations of 4-AP which cause an  $\sim 80\%$  block of the slow AHP in CA1 neurons also increase  $pH_i$  and  $\beta_T$  [44] as well as  $Ca^{2+}$  influx and burst firing [1]. Alternatively, weak permeation of the protonated forms of  $NH_3$  or TMeA through  $Ca^{2+}$ -activated  $K^+$  channels (including apamin-sensitive SK channels; [35]) would reduce  $I_{AHP}$  and, possibly,  $sI_{AHP}$  and could also contribute to the development of an ADP in the presence of  $NH_3$  or TMeA.

In summary, the weak bases  $NH_3$  and TMeA are widely used to investigate the effects of increases in  $pH_i$  on cellular behaviour. However, of the effects examined in the present study, only weak-base-induced increases in  $Ca^{2+}$  influx were attenuated by increasing  $\beta_T$  and, thus, can be attributed at least in part to an increase in  $pH_i$ . In contrast, the effects of  $NH_3$  and TMeA to reduce  $V_m$  and  $R_{in}$  and inhibit the medium and slow AHPs, and their underlying currents appeared independent of changes in  $pH_i$ . These actions may need to be taken into consideration when interpreting the effects of the external application of weak bases on neuronal excitability and function.

**Acknowledgments** We thank the Heart and Stroke Foundation of British Columbia and Yukon for financial support.

## References

- Andreasen M (2002) Inhibition of slow  $Ca^{2+}$ -activated  $K^+$  current by 4-aminopyridine in rat hippocampal CA1 pyramidal neurones. *Br J Pharmacol* 135:1013–1025
- Armstrong CM, Loboda A (2001) A model for 4-aminopyridine action on K channels: similarities to tetraethylammonium ion action. *Biophys J* 81:895–904
- Azouz R, Alroy G, Yaari Y (1997) Modulation of endogenous firing patterns by osmolarity in rat hippocampal neurones. *J Physiol (Lond)* 502:175–187
- Ballanyi K, Kaila K (1998) Activity-evoked changes in intracellular pH. In: Kaila K, Ransom BR (eds) *pH and Brain Function*. Wiley-Liss, New York, pp 291–308
- Billups B, Attwell D (1996) Modulation of non-vesicular glutamate release by pH. *Nature* 379:171–174
- Bonnet U, Wiemann M (1999) Ammonium prepulse: effects on intracellular pH and bioelectric activity of CA3-neurones in guinea pig hippocampal slices. *Brain Res* 840:16–22
- Boron WF, De Weer P (1976) Intracellular pH transients in squid giant axons caused by  $CO_2$ ,  $NH_3$ , and metabolic inhibitors. *J Gen Physiol* 67:91–112
- Braun AP (2001) Ammonium ion enhances the calcium-dependent gating of a mammalian large conductance, calcium-sensitive  $K^+$  channel. *Can J Physiol Pharmacol* 79:919–923
- Bruening-Wright A, Schumacher MA, Adelman JP, Maylie J (2002) Localization of the activation gate for small conductance  $Ca^{2+}$ -activated  $K^+$  channels. *J Neurosci* 22:6499–6506
- Byerly L, Moody WJ (1986) Membrane currents of internally perfused neurones of the snail, *Lymnaea stagnalis*, at low intracellular pH. *J Physiol (Lond)* 376:477–491
- Cai X, Liang CW, Muralidharan S, Kao JPY, Tang C-M, Thompson SM (2004) Unique roles of SK and  $Kv4.2$  potassium channels in dendritic integration. *Neuron* 44:351–364
- Chesler M (2003) Regulation and modulation of pH in the brain. *Physiol Rev* 83:1183–1221
- Chono K, Takagi H, Koyama S, Suzuki H, Ito E (2003) A cell model study of calcium influx mechanism regulated by calcium-dependent potassium channels in Purkinje cell dendrites. *J Neurosci Methods* 129:115–127
- Church J (1999) Effects of pH changes on calcium-mediated potentials in rat hippocampal neurons in vitro. *Neuroscience* 89:731–742
- Church J, McLennan H (1989) Electrophysiological properties of rat CA1 pyramidal neurones in vitro modified by changes in extracellular bicarbonate. *J Physiol (Lond)* 415:85–108
- Church J, Baxter KA, McLarnon JG (1998) pH modulation of  $Ca^{2+}$  responses and a  $Ca^{2+}$ -dependent  $K^+$  channel in cultured rat hippocampal neurones. *J Physiol (Lond)* 511:119–132
- Demaurex N, Grinstein S, Jaconi M, Schlegel W, Lew DP, Krause K-H (1993) Proton currents in human granulocytes: regulation by membrane potential and intracellular pH. *J Physiol (Lond)* 466:329–344
- Demaurex N, Orłowski J, Brisseau G, Woodside M, Grinstein S (1995) The mammalian  $Na^+ / H^+$  antiporters NHE-1, NHE-2, and NHE-3 are electroneutral and voltage independent but can couple to an  $H^+$  conductance. *J Gen Physiol* 106:85–111
- Fan P, Szerb JC (1993) Effects of ammonium ions on synaptic transmission and on responses to quisqualate and *N*-methyl-D-aspartate in hippocampal CA1 pyramidal neurons in vitro. *Brain Res* 632:225–231
- Inokuchi H, Yoshimura M, Polosa C, Nishi S (1993) Heterogeneity of the afterhyperpolarization of sympathetic preganglionic neurons. *Kurume Med J* 40:177–181
- Jung H-Y, Staff NP, Spruston N (2001) Action potential bursting in subicular pyramidal neurons is driven by a calcium tail current. *J Neurosci* 21:3312–3321
- Kelly T, Church J (2004) pH modulation of currents that contribute to the medium and slow afterhyperpolarizations in rat CA1 pyramidal neurones. *J Physiol (Lond)* 554:449–466
- Kiss L, Korn SJ (1999) Modulation of N-type  $Ca^{2+}$  channels by intracellular pH in chick sensory neurons. *J Neurophysiol* 81:1839–1847
- Lipton P (1999) Ischemic cell death in brain neurons. *Physiol Rev* 79:1431–1568
- Marcaggi P, Coles JA (2001) Ammonium in nervous tissue: transport across cell membranes, fluxes from neurons to glial cells, and role in signalling. *Prog Neurobiol* 64:157–183
- Martínez-Zaguilán R, Martínez GM, Lattanzio F, Gillies RJ (1991) Simultaneous measurement of intracellular pH and  $Ca^{2+}$  using the fluorescence of SNARF-1 and fura-2. *Am J Physiol* 260:C297–C307
- Martínez-Zaguilán R, Parnami G, Lynch RM (1996) Selection of fluorescent ion indicators for simultaneous measurements of pH and  $Ca^{2+}$ . *Cell Calcium* 19:337–349
- Mironov SL, Lux HD (1991) Cytoplasmic alkalization increases high-threshold calcium current in chick dorsal root ganglion neurones. *Pflügers Arch* 419:138–143
- Mironov SL, Lux HD (1993)  $NH_4Cl$ -induced inward currents and cytoplasmic  $Ca^{2+}$  transients in chick sensory neurones. *NeuroReport* 4:1055–1058
- Müller W, Connor JA (1991) Cholinergic input uncouples  $Ca^{2+}$  changes from  $K^+$  conductance activation and amplifies intradendritic  $Ca^{2+}$  changes in hippocampal neurons. *Neuron* 6:901–905
- Munsch T, Pape H-C (1999) Modulation of the hyperpolarization-activated cation current of rat thalamic relay neurones by intracellular pH. *J Physiol (Lond)* 519:493–504
- Ou-yang Y, Mellergård P, Siesjö BK (1993) Regulation of intracellular pH in single rat cortical neurons in vitro: a microspectrofluorometric study. *J Cereb Blood Flow Metab* 13:827–840
- OuYang YB, Mellergård P, Kristián T, Kristiánova V, Siesjö BK (1994) Influence of acid-base changes on the intracellular calcium concentration of neurons in primary culture. *Exp Brain Res* 101:265–271

34. Neher E (1992) Correction for liquid junction potentials in patch clamp experiments. *Methods Enzymol* 207:123–131
35. Park YB (1994) Ion selectivity and gating of small conductance  $\text{Ca}^{2+}$ -activated  $\text{K}^{+}$  channels in cultured rat adrenal chromaffin cells. *J Physiol (Lond)* 481:555–570
36. Ping HX, Shepard PD (1999) Blockade of SK-type  $\text{Ca}^{2+}$ -activated  $\text{K}^{+}$  channels uncovers a  $\text{Ca}^{2+}$ -dependent slow afterdepolarization in nigral dopamine neurons. *J Neurophysiol* 81:977–984
37. Roos A, Boron WF (1981) Intracellular pH. *Physiol Rev* 61:296–434
38. Shah M, Haylett DG (2000)  $\text{Ca}^{2+}$  channels involved in the generation of the slow afterhyperpolarization in cultured rat hippocampal pyramidal neurons. *J Neurophysiol* 83:2554–2561
39. Sheldon C, Cheng YM, Church J (2004) Concurrent measurements of the free cytosolic concentrations of  $\text{H}^{+}$  and  $\text{Na}^{+}$  ions with fluorescent indicators. *Pflügers Arch* 449:307–318
40. Somjen GG, Tombaugh GC (1998) pH modulation of neuronal excitability and central nervous system functions. In: Kaila K, Ransom BR (eds) pH and Brain function. Wiley-Liss, New York, pp 373–394
41. Stocker M (2004)  $\text{Ca}^{2+}$ -activated  $\text{K}^{+}$  channels: molecular determinants and function of the SK family. *Nat Rev Neurosci* 5:758–770
42. Storm JF (1990) Potassium currents in hippocampal pyramidal cells. *Prog Brain Res* 83:161–187
43. Sugiyama K, Muteki T (1994) Local anesthetics depress the calcium current of rat sensory neurons in culture. *Anesthesiology* 80:1369–1378
44. Szatkowski MS (1989) The effect of extracellular weak acids and bases on the intracellular buffering power of snail neurones. *J Physiol (Lond)* 409:103–120
45. Szatkowski MS, Thomas RC (1989) The intrinsic intracellular  $\text{H}^{+}$  buffering power of snail neurones. *J Physiol (Lond)* 409:89–101
46. Szerb JC, Butterworth RF (1992) Effect of ammonium ions on synaptic transmission in the mammalian central nervous system. *Prog Neurobiol* 39:135–153
47. Takahashi K-I, Dixon DB, Copenhagen DR (1993) Modulation of a sustained calcium current by intracellular pH in horizontal cells of fish retina. *J Gen Physiol* 101:695–714
48. Thomas RC (1984) Experimental displacement of intracellular pH and the mechanism of its subsequent recovery. *J Physiol (Lond)* 354:3P–22P
49. Tombaugh GC (1998) Intracellular pH buffering shapes activity-dependent  $\text{Ca}^{2+}$  dynamics in dendrites of CA1 interneurons. *J Neurophysiol* 80:1702–1712
50. Tombaugh GC, Somjen GG (1997) Differential sensitivity to intracellular pH among high- and low-threshold  $\text{Ca}^{2+}$  currents in isolated rat CA1 neurons. *J Neurophysiol* 77:639–653
51. Tombaugh GC, Somjen GG (1998) pH modulation of voltage-gated ion channels. In: Kaila K, Ransom BR (eds) pH and Brain Function. Wiley-Liss, New York, pp 395–416
52. Traynelis SF (1998) pH modulation of ligand-gated ion channels. In: Kaila K, Ransom BR (eds) pH and Brain Function. Wiley-Liss, New York, pp 417–446
53. Vogalis F, Storm JF, Lancaster B (2003) SK channels and the varieties of slow after-hyperpolarizations in neurons. *Eur J Neurosci* 18:3155–3166
54. Willoughby D, Schwiening CJ (2002) Electrically evoked dendritic pH transients in rat cerebellar Purkinje cells. *J Physiol (Lond)* 544:487–499
55. Wong RK, Prince DA (1978) Participation of calcium spikes during intrinsic burst firing in hippocampal neurons. *Brain Res* 159:385–390
56. Wu WW, Chan CS, Disterhoft JF (2004) Slow afterhyperpolarization governs the development of NMDA receptor-dependent afterdepolarization in CA1 pyramidal neurons during synaptic stimulation. *J Neurophysiol* 92:2346–2356
57. Yue C, Yaari Y (2004) KCNQ/M channels control spike afterdepolarization and burst generation in hippocampal neurons. *J Neurosci* 24:4614–4624